

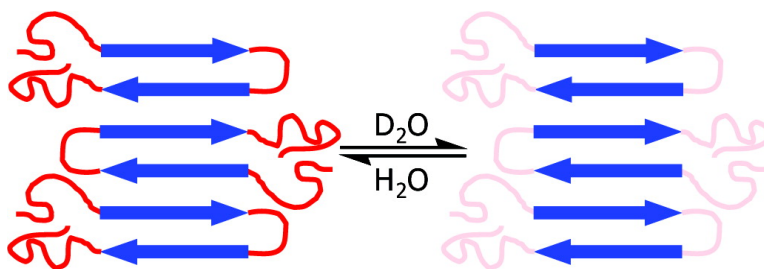
Communication

**Probing the Cross- $\beta$  Core Structure of Amyloid Fibrils by Hydrogen–Deuterium Exchange Deep Ultraviolet Resonance Raman Spectroscopy**

Ming Xu, Victor Shashilov, and Igor K. Lednev

*J. Am. Chem. Soc.*, **2007**, 129 (36), 11002-11003 • DOI: 10.1021/ja073798w • Publication Date (Web): 18 August 2007

Downloaded from <http://pubs.acs.org> on February 14, 2009



**More About This Article**

Additional resources and features associated with this article are available within the HTML version:

- Supporting Information
- Links to the 3 articles that cite this article, as of the time of this article download
- Access to high resolution figures
- Links to articles and content related to this article
- Copyright permission to reproduce figures and/or text from this article

[View the Full Text HTML](#)

## Probing the Cross- $\beta$ Core Structure of Amyloid Fibrils by Hydrogen–Deuterium Exchange Deep Ultraviolet Resonance Raman Spectroscopy

Ming Xu, Victor Shashilov, and Igor K. Lednev\*

Department of Chemistry, University at Albany, State University of New York, 1400 Washington Avenue, Albany, New York 12222

Received May 25, 2007; E-mail: lednev@albany.edu

Studying the structure of amyloid fibrils is important for the detailed understanding of fibrillogenesis at a molecular level. Amyloid fibrils are noncrystalline and insoluble, and thus are not amenable to conventional X-ray crystallography and solution NMR, the classical tools of structural biology.<sup>1</sup> Several specialized techniques with less general capabilities have been developed and utilized for probing fibrillar structure. Transmission electron microscopy (TEM) and scanning probe microscopy (SPM) provide general information on fibril topology and morphology including the length, width, interstrand spacing, the number of protofilaments, and the way they are assembled to form the fibril.<sup>1,2</sup> The application of fiber X-ray diffraction and scattering has been limited to short peptides mimicking the core structure of the fibrils formed from amyloidogenic protein.<sup>3–5</sup> Wide-angle X-ray scattering from flow-oriented fibrils has been utilized to estimate interstrand and intersheet spacing in cross- $\beta$  structures.<sup>6</sup> Solid-state NMR probes interatomic distances and torsion angles, which define local secondary structure and side-chain conformations. This technique, however, requires site-specific <sup>13</sup>C and/or <sup>15</sup>N labels.<sup>7</sup> Further, FTIR combined with proteolysis has been used to characterize the core structure of lysozyme fibrils.<sup>8</sup> Application of FTIR, however, is limited because of intense IR absorption by water. Here we report on the first application of hydrogen–deuterium exchange (HX) deep UV resonance Raman (DUVRR) spectroscopy to probe the secondary structure of the fibril cross- $\beta$  core. The amide I bandwidth in the DUVRR spectrum of the highly ordered cross- $\beta$  sheet was found comparable to that of the Gly–Gly crystal, indicating no inhomogeneous broadening due to various amino acid residues involved into the cross- $\beta$  core. This is in contrast to the Raman spectra of native globular protein  $\beta$ -sheets which exhibit broader Raman peaks than those of homopolypeptides.<sup>9,10</sup> The dominating spectral contribution was assigned to the antiparallel  $\beta$ -sheet. Thus, HX-DUVRR spectroscopy is a powerful tool for structural characterization of cross- $\beta$  core of amyloid fibrils.

HX is a valuable tool for characterizing protein structure, solvation, and water exposure, when combined with NMR,<sup>11</sup> mass spectrometry,<sup>12</sup> and vibrational spectroscopy.<sup>13</sup> In an amino acid residue, the main chain NH group and O, N, and S bound protons exchange easily, whereas carbon-bound hydrogens do not.<sup>14</sup> In the protein hydrophobic core or strongly hydrogen-bonded secondary structures, the HX rates are strongly reduced owing to shielding of exchangeable sites.<sup>13</sup> We hypothesized that amide N–H protons in unordered fragments of amyloid fibrils should exchange readily, whereas those hidden from water in the cross- $\beta$  structure will remain protonated. As shown by Mikhonin and Asher,<sup>15</sup> HX causes a downshift of the amide II DUVRR band from  $\sim 1555$  to  $\sim 1450$   $\text{cm}^{-1}$  (amide II') and the virtual disappearance of the amide III band in an unordered protein. Figure 1a illustrates corresponding spectral changes in the DUVRR signature of lysozyme upon deuteration.

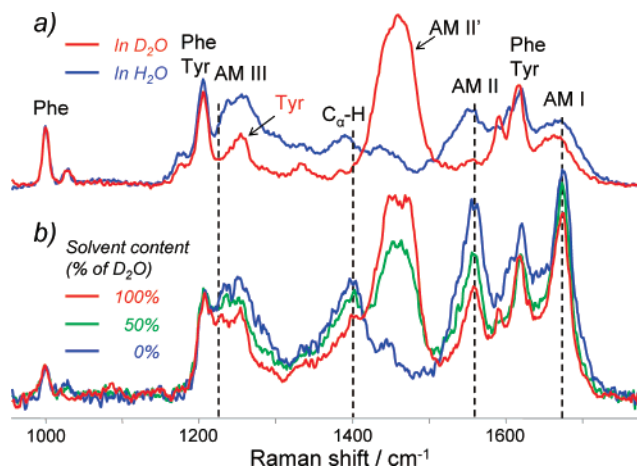


**Figure 1.** DUVRR spectra of (a) thermally denatured hen egg white lysozyme in H<sub>2</sub>O (blue) and D<sub>2</sub>O (red), and (b) lysozyme fibrils in H<sub>2</sub>O (blue), 50% D<sub>2</sub>O/H<sub>2</sub>O mixture (green), and 100% D<sub>2</sub>O (red). Excitation, 197 nm; AM, amide.

We hypothesized and then proved experimentally that DUVRR amide bands of the protonated cross- $\beta$  core remain unchanged (Figure 1b). Thus, the HX-DUVRR spectroscopic method will resolve the spectroscopic signature of the cross- $\beta$  core from that of water accessible moieties including unordered structures and  $\beta$ -turns.

The Bayesian approach<sup>16</sup> was utilized for the mathematical separation of overlapping DUVRR bands of the deuterated unordered moieties and the protonated cross- $\beta$  core. The dataset consisted of DUVRR spectra of lysozyme fibrils suspended in D<sub>2</sub>O/H<sub>2</sub>O mixture with D<sub>2</sub>O concentration ranging from 0% to 100% at 2% increments (selected spectra are shown in Figure 1b). The spectra of three pure components (cross- $\beta$  core and the protonated and the deuterated moieties) were sought using all prior information such as concentration profiles and spectral features of the pure components. The resolved DUVRR spectrum of the lysozyme fibril cross- $\beta$  core (Figure 2) is dominated by sharp amide I (1674  $\text{cm}^{-1}$ ), amide II (1559  $\text{cm}^{-1}$ ), C $_{\alpha}$ -H (1400  $\text{cm}^{-1}$ ), and amide III (1224  $\text{cm}^{-1}$ ) bands.

The ultimate goal of this study is to deduce structural information about the cross- $\beta$  core of lysozyme fibrils from the obtained spectral data. Approximate  $D_2$  symmetry of the antiparallel  $\beta$ -sheet gives rise to four vibrational modes in the amide I region, **A** (1675  $\text{cm}^{-1}$ ), **B** ( $\sim 1690$   $\text{cm}^{-1}$ , not observed), **B**<sub>2</sub> (1633  $\text{cm}^{-1}$ ), and **B**<sub>3</sub> (unknown).<sup>17</sup> Two of them, **A** (1675  $\text{cm}^{-1}$ ) and **B**<sub>2</sub> (1635  $\text{cm}^{-1}$ ), are well resolved in the cross- $\beta$  core spectrum indicating that the antiparallel  $\beta$ -sheet structure dominates the lysozyme fibril core. The other two amide I bands may be obscured by the strong 1675  $\text{cm}^{-1}$  band resonantly enhanced via Albrecht A term.<sup>17</sup> The C $_{\alpha}$ -H band is composed of at least three narrow sub-bands centered at

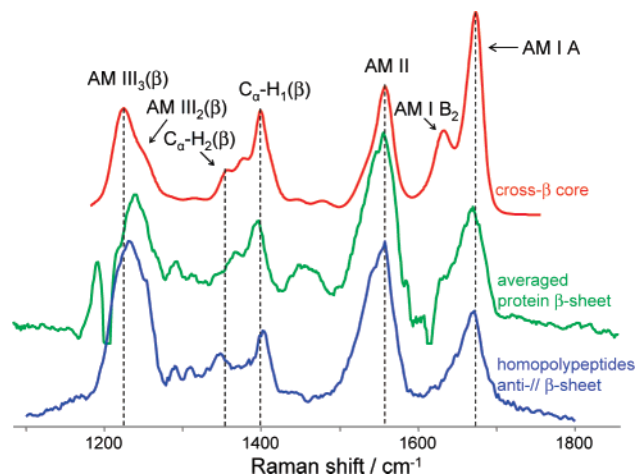


**Figure 2.** Pure DUVRR spectra of cross- $\beta$  core and the  $\beta$ -sheet structure of globular protein<sup>9</sup> and homopolypeptides.<sup>10</sup>

1400, 1377, and 1356  $\text{cm}^{-1}$ . Two of them, 1400 and 1356  $\text{cm}^{-1}$ , are observed in the  $\beta$ -sheet region of poly-L-lysine spectra and originate from  $\text{C}_{\alpha}\text{-H}$  in-plane and out-of-plane vibrations. This assignment was made based on MP2/TZV(d,p) normal-mode analysis followed by the resonance Raman enhancement calculation of 2-amino-*N*-methylacetamide ( $\text{NH}_3\text{CH}_2\text{CONHCH}_3$ , ANMA), the well-accepted model for the protein amide group.<sup>18</sup> In addition, we constrained the  $\Psi$  dihedral angle of ANMA to  $135^\circ$  to mimic the geometry of amide motifs of the antiparallel  $\beta$ -sheet. The origin of the 1376  $\text{cm}^{-1}$  band is yet to be clarified. The amide III band is dominated by a  $\sim 1224 \text{ cm}^{-1}$  band with a small shoulder at 1255  $\text{cm}^{-1}$ . Both bands originate predominantly from C–N stretching and N–H stretching. The former is strengthened because of the coupling with  $\text{C}_{\alpha}\text{-H}$  bending as evident from the MP2 calculation on the ANMA model.

As shown by Mikhonin et al.,<sup>19</sup> the average Ramachandran  $\Psi$  dihedral angle of the amide group can be calculated based on the band frequency of the amide III vibrational mode. For a multi-stranded  $\beta$ -sheet structure,<sup>19</sup>

$$\nu_{\text{amide III}}^{\beta}(\Psi) = (1244 \text{ (cm}^{-1}) - 54 \text{ (cm}^{-1})) \sin(\Psi + 26^\circ)$$

On the basis of the above equation, we estimate a  $\Psi$  angle of  $133^\circ$  for the cross- $\beta$  core structure. This value falls within the range of  $129\text{--}133^\circ$  that we estimated using the atomic-resolution X-ray structure (2OMP) of the antiparallel  $\beta$ -sheet fragment of the insulin fibril.<sup>4</sup> It is worth noting here that the DUVRR spectrum of insulin fibrils (not shown) is also very similar to that of lysozyme reported here despite the completely different mechanisms of fibrillation of the two proteins.

The pure DUVRR spectra of a  $\beta$ -sheet (with no contribution from  $\beta$ -turns) extracted by means of least-squares regression from DUVRR spectra of 12 proteins with known secondary structures<sup>9</sup> and an antiparallel  $\beta$ -sheet obtained from the mixture of poly-L-lysine (PLL) and poly-L-glutamic acid (PGA)<sup>10</sup> are also shown in Figure 2 for comparison. Table 1 summarizes the peak positions and bandwidths of all three  $\beta$ -sheet spectra. Although the band positions of all major bands are similar in all three spectra, amide I, amide II, and  $\text{C}_{\alpha}\text{-H}$  bands of the cross- $\beta$  core structure are significantly sharper than those in spectra of homopolypeptides and proteins (Figure 2 and Table 1). In particular, the bandwidth of the amide I band of the cross- $\beta$  core structure is more than twice narrower than that of globular proteins and homopolypeptide  $\beta$ -sheets (Table 1). This indicates that the regularity of the fibril

**Table 1.** Peak Positions and Band Widths (Full Width at Half Height, FWHH) of Main DUVRR Bands of Cross- $\beta$  Core,  $\beta$ -sheet of Globular Protein,<sup>9</sup> and Homopolypeptides<sup>10</sup>

	peak position (bandwidth, FWHH), $\text{cm}^{-1}$		
	cross- $\beta$ core	globular proteins <sup>9</sup>	homopolypeptides <sup>10</sup>
amide I	1674 (17)	1671 (43)	1671 (35)
amide II	1558 (31)	1557 (53)	1557 (46)
$\text{C}_{\alpha}\text{-H}$	1400 (23)	1397 (30)	1402 (25)
amide III	1225 (40)	1241 (57)	1231 (54)

cross- $\beta$  core is higher than that of polypeptide  $\beta$ -structure. The 17  $\text{cm}^{-1}$  bandwidth for the fibril core amide I band is close to the value reported for the UV Raman spectrum of Gly–Gly crystal.<sup>20</sup> This result is in contrast to vast experimental data showing that proteins adopt less uniform secondary structures as compared to that of homo-polypeptides, to accommodate the influence of various side chains. The lack of inhomogeneous broadening of the Raman bands because of various amino acid residues might indicate that the cross- $\beta$  core structure is independent of the protein sequence.

In conclusion, hydrogen–deuterium exchange combined with DUVRR spectroscopy provides structural information about fibrils which is not easily accessible by other techniques at the moment. Up to now, X-ray diffraction studies of the fibril cross- $\beta$  core have been performed only on microcrystals grown from short fibril-forming segments.<sup>3–5</sup> HX-DUVRR spectroscopy should allow for comparative characterization of the cross- $\beta$  core structure in the model short-peptide fibrils and those formed from an amyloidogenic protein. This study is ongoing in our laboratory.

**Acknowledgment.** We are grateful to Profs. B. Szaro and P. Toscano for valuable advice.

**Supporting Information Available:** Sample preparation, details on the Bayesian statistics, 2D-correlation analysis, and the abstract factor analysis. This material is available free of charge via the Internet at <http://pubs.acs.org>.

## References

- Chiti, F.; Dobson, C. M. *Annu. Rev. Biochem.* **2006**, *75*, 333–366.
- Mastrangelo, I. A.; Ahmed, M.; Sato, T.; Liu, W.; Wang, C.; Hough, P.; Smith, S. O. *J. Mol. Biol.* **2006**, *358*, 106–119.
- Nelson, R.; Sawaya, M. R.; Balbirnie, M.; Madsen, A. O.; Riek, C.; Grothe, R.; Eisenberg, D. *Nature (London)* **2005**, *435*, 773–778.
- Sawaya, M. R.; Sambashivan, S.; Nelson, R.; Ivanova, M. I.; Sievers, S. A.; Apostol, M. I.; Thompson, M. J.; Balbirnie, M.; Wiltzius, J. J.; McFarlane, H.; Madsen, A. O.; Riek, C.; Eisenberg, D. *Nature (London)* **2007**, *447*, 453–457.
- Inouye, H.; Sharma, D.; Goux, W. J.; Kirschner, D. A. *Biophys. J.* **2006**, *90*, 1774–1789.
- Squires, A. M.; Devlin, G. L.; Gras, S. L.; Tickler, A. K.; MacPhee, C. E.; Dobson, C. M. *J. Am. Chem. Soc.* **2006**, *128*, 11738–11739.
- Tycko, R. *Q. Rev. Biophys.* **2006**, 1–55.
- Frare, E.; Mossuto, M. F.; Laureto, P. P. d.; Dumoulin, M.; Dobson, C. M.; Fontana, A. *J. Mol. Biol.* **2006**, *361*, 551–561.
- Huang, C.-Y.; Balakrishnan, G.; Spiro, T. G. *J. Raman. Spectrosc.* **2006**, *37*, 277–282.
- Mikhonin, A. V.; Myshakina, N. S.; Bykov, S. V.; Asher, S. A. *J. Am. Chem. Soc.* **2005**, *127*, 7712–7720.
- Henkels, C. H.; Oas, T. G. *J. Am. Chem. Soc.* **2006**, *128*, 7772–7781.
- Kheterpal, I.; Wetzel, R. *Acc. Chem. Res.* **2006**, *39*, 584–593.
- DeFlores, L. P.; Tokmakoff, A. *J. Am. Chem. Soc.* **2006**, *128*, 16520–16521.
- Englander, S. W.; Sosnick, T. R.; Englander, J. J.; Mayne, L. *Curr. Opin. Struct. Biol.* **1996**, *6*, 18–23.
- Mikhonin, A. V.; Asher, S. A. *J. Phys. Chem. B* **2005**, *109*, 3047–3052.
- Knuth, K. In *SPIE '98 Proceedings: Bayesian Inference for Inverse Problems*; SPIE: San Diego, CA, July, 1998; Vol. 3449, pp 147–158.
- Tsuboi, M.; Kubo, Y.; Akahane, K.; Benevides, J. M.; Thomas, G. J., Jr. *J. Raman Spectrosc.* **2006**, *37*, 240–247.
- Asher, S. A.; Ianoul, A.; Mix, G.; Boyden, M. N.; Karnoup, A.; Diem, M.; Schweitzer-Stenner, R. *J. Am. Chem. Soc.* **2001**, *123*, 11775–11781.
- Mikhonin, A. V.; Bykov, S. V.; Myshakina, N. S.; Asher, S. A. *J. Phys. Chem. B* **2006**, *110*, 1928–1943.
- Pajcini, V.; Chen, X. G.; Bormett, R. W.; Geib, S. J.; Li, P.; Asher, S. A.; Lidiak, E. G. *J. Am. Chem. Soc.* **1996**, *118*, 9705–9715.

JA073798W